Biophysical Chemistry 190–191 (2014) 8–16

Contents lists available at ScienceDirect

Biophysical Chemistry

journal homepage: http://www.elsevier.com/locate/biophyschem

EPR analysis of cyanide complexes of wild-type human neuroglobin and mutants in comparison to horse heart myoglobin

Sabine Van Doorslaer [a,*], Florin Trandafir [a], Jeffrey R. Harmer [b], Luc Moens [c], Sylvia Dewilde [c]

[a] SIBAC Laboratory, Department of Physics, University of Antwerp, Antwerp, Belgium
[b] Centre for Advanced Imaging, University of Queensland, St Lucia, QLD, 4072, Australia
[c] PPES Laboratory, Department of Biomedical Sciences, University of Antwerp, Antwerp, Belgium

HIGHLIGHTS

- First reported EPR study of cyanide-ligated neuroglobins.
- First determination of the full ^{13}C hyperfine tensor of the cyanide carbon in a cyanide-ligated globin.
- Disagreement of ^{13}C hyperfine data of cyanide-ligated myoglobin with predictions from NMR reveal flaws in theortical model.
- The present ^{13}C hyperfine data challenge the current interpretation of ^{13}C NMR shifts in cyanide-ligated haem proteins.

GRAPHICAL ABSTRACT

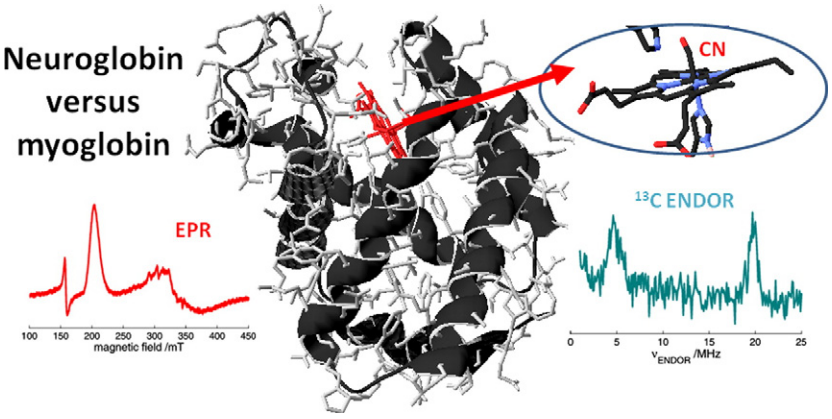

ARTICLE INFO

Article history:
Received 20 February 2014
Received in revised form 21 March 2014
Accepted 28 March 2014
Available online 8 April 2014

Keywords:
Neuroglobin
Electron paramagnetic resonance
Cyanide binding

ABSTRACT

Electron paramagnetic resonance (EPR) data reveal large differences between the ferric (^{13}C-)cyanide complexes of wild-type human neuroglobin (NGB) and its H64Q and F28L point mutants and the cyanide complexes of mammalian myo- and haemoglobin. The point mutations, which involve residues comprising the distal haem pocket in NGB, induce smaller, but still significant changes, related to changes in the stabilization of the cyanide ligand. Furthermore, for the first time, the full ^{13}C hyperfine tensor of the cyanide carbon of cyanide-ligated horse heart myoglobin (hhMb) was determined using Davies ENDOR (electron nuclear double resonance). Disagreement of these experimental data with earlier predictions based on ^{13}C NMR data and a theoretical model reveal significant flaws in the model assumptions. The same ENDOR procedure allowed also partial determination of the corresponding ^{13}C hyperfine tensor of cyanide-ligated NGB and H64QNGB. These ^{13}C parameters differ significantly from those of cyanide-ligated hhMb and challenge our current theoretical understanding of how the haem environment influences the magnetic parameters obtained by EPR and NMR in cyanide-ligated haem proteins.

* Corresponding author at: University of Antwerp, Department of Physics, Universiteitsplein 1, B-2610 Wilrijk-Antwerp, Belgium. Tel.: +32 32652461; fax: +32 32652470.
E-mail address: sabine.vandoorslaer@uantwerpen.be (S. Van Doorslaer).

http://dx.doi.org/10.1016/j.bpc.2014.03.007
0301-4622/

1. Introduction

Since its discovery in 2000 [1], neuroglobin (Ngb) has been intensively studied. This haem-containing globular protein has the typical globin fold consisting of 8 α-helices (A to H) and it is expressed in the brain of a variety of vertebrates, such as mammals, fish, amphibians, birds and reptiles [1–4]. It has about 25% sequence identity with vertebrate haemoglobin (Hb) and myoglobin (Mb) [5]. Interestingly, it is retained in the Antarctic icefish *Chaenocephalus aceratus* that lacks Hb and Mb [6]. The physiological role of Ngb is still unclear [7]. Possible involvement in protection against apoptosis, removal of reactive oxygen or nitrogen species and a role in ligand sensing have been proposed [7].

In the absence of exogenous ligands, the haem iron in the ferric and ferrous forms of Ngb is ligated to two histidines, namely His96 at position 8 of the F-helix, which is highly conserved in all globins, and His64 at position E7 on the distal side of the haem [8–11] (supplementary information, Fig. S1). This hexa-coordination of the haem-iron contrasts to ferrous mammalian Hb and Mb, in which the haem is only ligated to F8His leaving the distal side open for coordination of exogenous ligands. Due to competition with the endogenous distal HisE7, Ngb shows a slower binding of exogenous ligands, although the intrinsic affinity of the penta-coordinated form to bind O_2 and CO is quite high [12–14]. Moreover, in ferrous human neuroglobin (NGB), the His-binding affinity is found to decrease by a factor of ten due to a disulfide-bridge formation between Cys55 (position 5 of the D helix) and Cys46 (at position 7 of the loop connecting helices C and D) [13]. This leads to a concomitant increase in the O_2 affinity, suggesting that the release of O_2 in NGB is regulated by the redox state of the disulfide bridge. Formation of the disulfide bridge is found to alter the haem-pocket structure [15], a process in which Phe28 (position B10) plays an important role [16].

A crystallographic study revealed that an unusual sliding motion of the haem occurs when CO ligates to the ferrous haem of murine Ngb (mNgb) [17]. Although molecular dynamics (MD) simulations corroborate the haem-sliding ability [18,19], MD simulations comparing crystal and solution conditions also revealed that the experimentally observed dynamics of the haem group may be affected by the crystal packing [18]. Since the Fe(III)–CN^- complex in ferric cyanide-ligated globins is believed to be isostructural and isoelectronic to the Fe(II)–CO complex, it comes as no surprise that cyanide binding to Ngb and related mutants has been investigated [14,20–23]. Except for the cyanide-affinity determination of NGB [14], all currently reported information on cyanide-ligated Ngb variants is based on NMR studies [20–23]. NMR data revealed haem orientational disorder in ferric wild-type (wt) mNgb [20] and NGB [24] and in cyanide-ligated forms of ferric wild-type NGB [23], mNgb [20] and related mutants [22,23]. The disorder consists of a 180° haem rotation about the α–γ-meso axis (see Fig. S2, supplementary material). The cyanide ligation rate is faster for one of the two haem orientations ([20,23], Table S1). In NGB, this is attributed to the lower stability of the distal His-iron coordination bond and a reduced steric hindrance at the bottom of the haem cavity in this conformer, allowing for haem sliding [23]. The haem orientational disorder is found to persist in the H64Q/V68F mNgb double mutant [22]. Formation of the earlier mentioned disulfide bridge in NGB also influences the cyanide binding rate [23].

Although electron paramagnetic resonance (EPR) has often been used to characterize ferric cyanide-ligated globins [25–31], no EPR data of cyanide-ligated Ngbs have been reported so far. In the present work, continuous-wave (CW) and pulsed EPR techniques are used to investigate the cyanide-ligated ferric form of wild-type NGB and its H64Q and F28L mutants (mutations on positions E7 and B10, respectively). The mutants were chosen to test the influence of two key amino acids in the distal haem-pocket region. All findings are compared in detail with reported EPR data on other cyanide-ligated ferric globin forms. Furthermore, although ^{13}C NMR of the iron-bound cyanide in ferric cyanide complexes of haem proteins has been shown to reveal important information about the haem reactivity [32–35], only a few studies have attempted to determine the full ^{13}C hyperfine tensor of the cyanide carbon of such haem complexes [26,36]. Here, Davies ^{13}C-ENDOR is applied to extract information on this tensor for cyanide-ligated NGB variants in comparison to those of the cyanide complex of horse heart myoglobin (hhMb-CN).

2. Materials and methods

2.1. Cloning, expression and purification of NGB and its H64Q and F29L mutants

The QuickChangeTM site-directed mutagenesis method (Stratogene) was used to make the F28LNGB and H64QNGB mutants as described earlier [16,37]. Expression of wt NGB and its mutants was done as reported earlier [8]. In short, the plasmids (cDNA cloned in pET3a) were transformed into *E. Coli* strain BL21(DE3)pLysS. Cells were grown at 25 °C in a TB medium containing 1.2% bactotryptone, 2.4% yeast extract, 0.4% glycerol, 72 mM potassium phosphate buffer, pH 7.5, 200 μg/ml ampicillin, 30 μg/ml chloramphenicol and 1 mM δ-amino-levulinic acid. After induction, the cells were grown overnight, and subsequently harvested, resuspended in lysis buffer (50 mM Tris–HCl, pH 8.0, 0.1 mM EDTA, 0.6 mM dithiothreitol) and exposed to three freeze–thaw steps. Sonication was used until the cells completely lysed. The extract was clarified by low (10 min at 10,000 *g*) and hi% gh (60 min at 105,000 × *g*) speed centrifugation. The obtained supernatant was collected and fractionated by 60 ammonium sulfate precipitation. The pellets were dialyzed against 5 mM Tris–HCl, pH 8.5 and loaded onto DEAE-Sepharose Fast Flow column for ion exchange chromatography. The wt NGB or NGB mutant (F28L or H64Q) was eluted with 200 mM NaCl from the sepharose. The NGB fractions (wt, F28L or H64Q) were concentrated by Amicon filtration (PM10) and passed through a sephacryl S200 column for gel filtration. They were then stored at −20 °C. SDS-PAGE screening was done for testing the protein purity.

2.2. Preparation of the ferric cyanide-ligated forms

Ferric horse heart myoglobin (hhMb) was puchased from Sigma-Aldrich as lyophilized powder. This powder was then dissolved in a 50 mM Tris–HCl buffer at pH 8.0. KCN (all nuclei in natural abundance) and $K^{13}CN$ were bought from Sigma-Aldrich. The ferric cyanide-ligated forms of the NGB variants and of hhMb were prepared by adding a 40 times excess of KCN or $K^{13}CN$ to the ferric proteins. Formation of the cyanide-ligated form was checked by optical absorption spectroscopy. For EPR measurements, 20 wt.% of the cryoprotectant glycerol was added. Final concentrations were ca. 2 mM for hhMb-CN, 0.8–1 mM for NGB-CN and H64QNGB-CN, and ~0.4 mM for F28LNGB-CN (and their analogues with $^{13}CN^-$).

2.3. EPR spectroscopy

X-band CW-EPR measurements were performed on a Bruker ESP 300E spectrometer (microwave frequency 9.44 GHz) equipped with a liquid Helium cryostat (Oxford Inc.). EPR spectra were obtained with a modulation frequency of 100 kHz, a modulation amplitude of 0.5 mT and a microwave power of 1 mW at a temperature of 10 K.

X-band pulsed EPR experiments were performed at 7 K on a Bruker Elexsys instrument equipped with Helium cryostat (Oxford Inc.).

Single matched resonance transfer hyperfine sublevel correlation (SMART-HYSCORE) experiments were performed using the sequence HTA-t_1-π-t_2-HTA-τ-π-τ-*echo* [38] with a high-turning angle (HTA) pulse of length 32 ns, a π pulse of 16 ns and a τ value of 120 ns. A microwave field strength of 15.625 MHz was used. The HYSCORE traces were baseline corrected using a third-order polynomial, apodized with a Hamming window and zero-filled. After Fourier transformation absolute-value spectra were computed.

Davies ENDOR (electron nuclear double resonance) experiments [39] were performed using the microwave pulse sequence π-*T*-π/2-*τ*-π-*τ*-*echo* with $t_{\pi/2} = 16$ ns, $t_{\pi} = 32$ ns, $\tau = 110$ ns. During time T (= 4.5 μs), a radio-frequency pulse of 3 μs was inserted. A 500 W rf amplifier (500A100A, Amplifier Research) was used at 50% of its full power.

The EasySpin program was utilized to simulate all EPR spectra [40].

3. Results

3.1. CW-EPR analysis

Fig. 1 shows the low-field part of the X-band CW-EPR spectra of the cyanide-ligated forms of the NGB variants along with the corresponding simulations using the *g* values listed in Table 1. In line with observations for other cyanide-haem complexes [28,29,41], the EPR spectra are typical for so-called HALS (highly anisotropic low-spin) complexes where $g_z > 3.1$ and the high-field (g_x) feature is not observable in the X-band CW-EPR spectra due to the large *g*-strain effects. Although the overall *g* anisotropy seems to be smaller for the cyanide complexes of the NGB wt and mutants than for vertebrate haemo- and myoglobins, the *g*-strain effects are considerably larger than found for the earlier studied cyanide complex of hhMb [31]. This seems to be the reason why no clear electron spin echo signal could be observed at higher field for the cyanide-ligated complexes of the NGB variants in contrast to the hhMb-CN case (see supplementary material, Fig. S3). Furthermore, the principal *g* values of ferric NGB-CN, H64QNGB-CN and F28LNGB-CN clearly differ (Table 1), reflecting the effect of the mutations, as will be discussed in Section 4.

3.2. ^{13}C-Davies ENDOR experiments

Work by the Fujii group [32–35] suggests that the ^{13}C NMR shift of the cyanide carbon in cyanide-ligated haem proteins can be linked to the donor effect of the proximal imidazole. Although the origin of the observed ^{13}C NMR shift is the same as that of the ^{13}C hyperfine interaction addressable by ENDOR techniques, only few studies have attempted to obtain this information for ferric cyanide complexes of haem proteins [26,36]. To our knowledge, the only determination of a full ^{13}C hyperfine tensor for such a system, is the one performed for cyanide-ligated cytochrome P450cam [36]. For cyanide-ligated globins, only the study of Mulks et al. [26] reports a partial determination of the hyperfine tensor for the swMb-CN and hHb-CN cases. The reason is clear: due to the high *g*-anisotropy and large *g* strain and corresponding weak (or not detectable) high-field EPR feature ($g = g_x$), ENDOR spectroscopy becomes challenging. In fact, it is not surprising that the only full determination of the ^{13}C hyperfine tensor is performed for cytochrome P450cam, because its cyanide complex exhibits a much smaller *g*-anisotropy than the corresponding cyanide complexes of globins (Table 1).

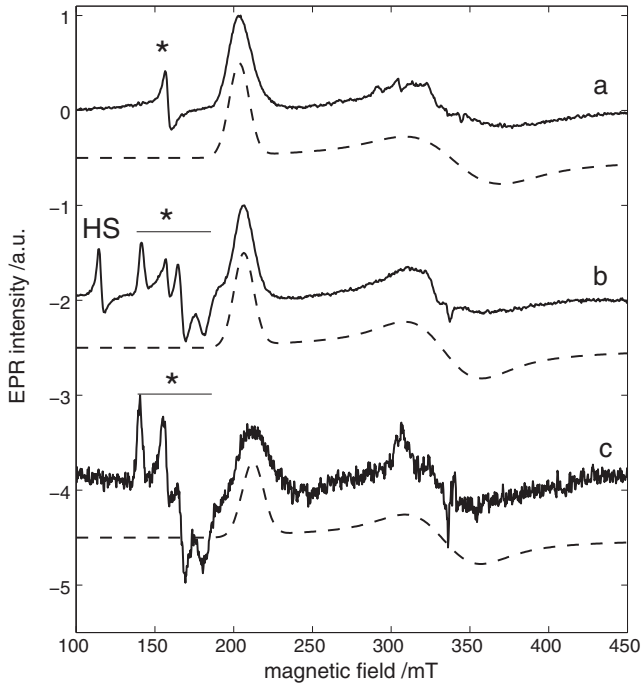

Fig. 1. Low-field region of the X-band CW-EPR spectra of frozen solutions of ferric (a) NGB-CN, (b) H64QNGB-CN and (c) F28LNGB-CN. The dashed lines represent the corresponding simulations using the parameters given in Table 1. The asterisk indicates signals stemming from non-haem iron. In spectrum (b) an additional signal is present due to a small fraction of the high-spin (HS) form of ferric H64QNGB (indicated as HS in the figure).

Since an electron spin echo could be observed at high field for hhMb-^{13}CN (see supplementary material, Fig. S3), this ferric cyanide-globin complex is the most suitable candidate to attempt a full determination of the hyperfine tensor of the cyanide carbon. ^{13}C Davies ENDOR signals could indeed be observed at different magnetic-field setting allowing for a full hyperfine analysis (Fig. 2, Table 2). Similar experiments were also set up for ferric H64QNGB-^{13}CN (Fig. 3) and NGB-^{13}CN (Fig. 4). One of the ENDOR lines at the low-field ($g = g_z$) position of H64QNGB-^{13}CN (Fig. 3a) is overlapping with the ^{1}H ENDOR signal. Therefore, the corresponding ENDOR spectrum of H64QNGB-CN was recorded (Fig. 3b), allowing identification of the ^{13}C ENDOR contribution in the difference spectrum. While the ENDOR lines could be followed till the $g = g_y$ position for ferric H64QNGB-^{13}CN (Fig. 3), the ENDOR spectrum could only be observed at the lowest field setting for ferric NGB-^{13}CN (Fig. 4), leading to only partial determination of the hyperfine tensor. Similar experiments were attempted for F28LNGB-^{13}CN, but the overall signal intensity was too low.

As mentioned, the g strain is considerably larger for the NGB-CN proteins than for hhMb-CN. Similarly, the ^{13}C-ENDOR lines are broader (compare Figs. 3 and 4 with Fig. 2). One source of this broadening is freezing-induced strain effects. Since the haem is very close to the protein surface in the globins, strains induced by the freezing solvent could easily lead to small local fluctuations in the haem environment, resulting in different complexes in frozen solution with slightly different magnetic parameters. However, this effect is expected to be similar for the NGB and Mb variants. ^{1}H-NMR reveals, however, haem orientational disorder in all cyanide-ligated Ngbs (presence of two conformers with a 180° haem rotation about the α–γ-meso axis) [20–23]. It is not unreasonable that the EPR parameters of these two conformers differ slightly, contributing to the increased overall line width. Furthermore, an intramolecular disulfide bridge can be formed in NGB with a concomitant clear change in the EPR parameters of wild-type ferric NGB [15]. Although only one EPR contribution due to a low-spin haem is observed for NGB-CN, the co-existence of proteins with and without the disulfide bridge may contribute to the observed line broadening. Indeed, disulfide-bridge formation was found to affect the cyanide binding kinetics [23]. Finally, MD simulations reveal that the structural rearrangements of loops CD and EF have an influence on the haem pocket [19]. The structure of these loops can be affected by the freezing, increasing the strain effects observed in the EPR spectra.

3.3. ^{14}N-SMART-HYSCORE spectra

Our earlier work on the cyanide complexes of hhMb and protoglobin variants [31] showed that the z-component of the ^{14}N hyperfine interaction of the haem nitrogens is sensitive to the electronic ground state, more particularly, a decrease in this hyperfine coupling has been associated with an increase in the relative contribution of the d_{xy} orbital to the molecular orbital containing the unpaired electron. SMART-HYSCORE experiments at the g_z observer position allowed for a clear determination of two haem nitrogen contributions showing that the haem

Table 1
Principal g values of frozen solutions of ferrric NGB-CN, H64QNGB-CN and F28LNGB-CN in comparison with those reported for other cyanide-ligated complexes of globins and haem proteins. For the globin proteins the amino acids at the key positions B10, E7 and E11 are indicated. The globins are subdivided in two categories: "bis-His" = globins having a haem iron ligated to two His in its ferric state in the absence of exogenous ligands, and "other" = other ligation types in the ferric state. n.d. = not determined. *Dm*Hb = *Drosophila melanogaster* haemoglobin, swMb = sperm whale myoglobin, hHb = human haemoglobin, *Lp*Hb = *Lucina pectinata* haemoglobin, Pgb* = Cys → Ser mutant of protoglobin, *Chlam*Hb = *Chlamydomonas* haemoglobin, sb legHb = soyabean leghaemoglobin, NP4 = nitrophorin-4, Cyt = cytochrome.

Cyanide complex of	g_x	g_y	g_z	B10	E7	E11	Ref.
	I. Globins bis-His						
NGB	n.d.	1.97 ± 0.01	3.295 ± 0.005	Phe	His	Val	This work
F28LNGB	n.d.	2.01 ± 0.01	3.16 ± 0.01	Leu	His	Val	This work
Barley Hb	n.d.	n.d.	3.32	Phe	His	Val	[29]
	II. Globins other						
H64QNGB	n.d.	2.01 ± 0.01	3.250 ± 0.005	Phe	Gln	Val	This work
swMb	0.93	1.871	3.442	Leu	His	Val	[25]
hhMb	≤0.92	1.82	3.420	Leu	His	Val	[31]
hHb	0.75	1.88	3.41	Leu	His	Val	[42]
*Lp*Hb I	n.d.	n.d.	3.29	Phe	Gln	Phe	[30]
*Lp*Hb II	n.d.	n.d.	3.23	Tyr	Gln	Phe	[30]
Pgb*	≤0.99	2.08	2.91	Tyr	Val	Phe	[31]
F145WPgb*	≤0.96	2.10	3.015	Tyr	Val	Phe	[31]
*Aplysia*Mb	n.d.	2.0	3.5	Leu	Val	Ile	[43]
*Chlam*Hb	n.d.	n.d.	3.19	Tyr	Gln	Gln	[28]
sb legHb	1.0	1.97	3.35	Tyr	His	Ala	[27]
	III. Other haem proteins — non globins						
NP4	n.d.	1.96	3.35	–	–	–	[44]
Cyt P450cam	1.8	2.28	2.63	–	–	–	[36]
Horse Cyt c	0.93	1.89	3.45	–	–	–	[45]
Lacto-peroxidase	1.56	2.25	2.92	–	–	–	[46]
Horseradish peroxidase	1.2	2.1	3.05	–	–	–	[47]

nitrogens are not magnetically equivalent (Fig. 5: H64QNGB-CN and supplementary material, Fig. S4: NGB-CN). The corresponding hyperfine and nuclear quadrupole values for these two contributions, determined by spectrum simulations, are compared to those of other systems in Table 3.

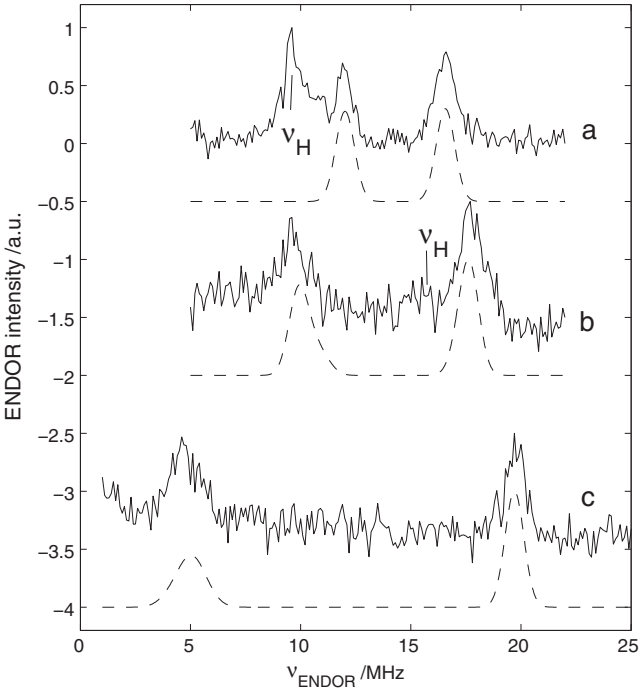

Fig. 2. Experimental (solid line) and simulated (dashed line) X-band Davies-ENDOR spectra of a frozen solution of ferric hhMb-^{13}CN taken at observer positions corresponding to (a) $g = g_z$, (b) $g = g_y$ and (c) $g = 0.925$ ($\sim g_x$) (B_0 = 749.7 mT, mW frequency 9.71 GHz). Only the ^{13}C ENDOR contributions are simulated using the parameters given in Table 2. ν_H indicates the position of the proton Larmor frequency.

4. Discussion

All EPR g-value data of the cyanide-ligated haem proteins presented in Table 1 are typical for what is, in an (over)simplified description, ascribed to an electron configuration $(d_{xy})^2(d_{xz}d_{yz})^3$ [41]. If all principal g values are known, they can be directly related to the ligand-field splitting parameters and allow for computation of the energy splitting between the ground and two excited Kramer doublets [41,48,49]. However, in many cases, the high-field feature of the EPR spectrum cannot be detected which prevents a detailed analysis of the energy splitting (as is the case for the NGB-cyanide complexes under study). Often, a rule of thumb ($g_x^2 + g_y^2 + g_z^2 = 16$) is used to derive the lowest g value [41]. However, this equation is not generally applicable and will lead to errors in the analyses. We therefore will not use it here to analyse the NGB data.

The principal g values of all cyanide complexes of the studied NGB proteins (*i.e.* g_z values of 3.16–3.32) differ strongly from those of mammalian Mb and Hb ($g_z \sim 3.4$–3.5). This is in agreement with the smaller values of the axial and rhombic anisotropy of the magnetic susceptibility tensor found by ^{1}H-NMR for ferric H64Q/V68FmNgb-CN compared to the cyanide complexes of vertebrate Mb and Hbs [22]. The magnetic susceptibility tensor determined by NMR correlates with the $\boldsymbol{g}$ tensor determined by EPR [50]. In the following, we will consider the factors that could possibly explain why the g_z values of NGB-CN and its mutants are much lower than those of MbCN and HbCN.

g_z values lower than 3.4 have been observed for cyanide complexes of different other globins and related haem proteins (Table 1). Our EPR

Table 2
^{13}C-hyperfine values of Mb-^{13}CN, NGB-^{13}CN and H64QNGB-^{13}CN determined by Davies ENDOR spectroscopy on frozen solutions. The values are compared with reported data on cyanide ligated haem proteins. n.d. = not detected.

	A_x/MHz	A_y/MHz	A_z/MHz	Reference
hhMb-^{13}CN	−23.0 (±0.6)	−27.6 (±0.4)	−28.7 (±0.2)	This work
NGB-^{13}CN	n.d.	n.d.	−22.5 (±1)	This work
H64QNGB-^{13}CN	n.d.	−25 (±1)	−23 (±1)	This work
swMb-^{13}CN	n.d.	n.d.	−28.64 (±0.08)	[26]
hHb-^{13}CN	n.d.	n.d.	−27.33 (±0.16)	[26]
Cyt P450-^{13}CN	−20.0	−18.6	−26.0	[36]

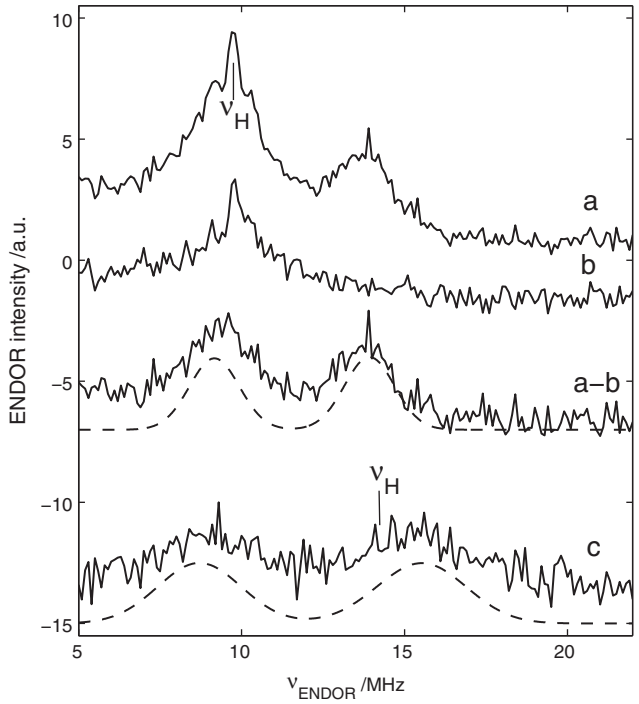

Fig. 3. Experimental X-band Davies ENDOR spectra of frozen solutions of ferric (a) H64QNGB-^{13}CN and (b) H64QNGB-CN taken at an observer position corresponding to g_z, and of ferric (c) H64QNGB-^{13}CN taken at an observer position corresponding with g_y. Data (a–b) shows the difference of the spectrum (a) minus (b), which represents the ^{13}C ENDOR contribution. Dashed lines show the simulations computed using parameters given in Table 2. ν_H indicates the position of the proton Larmor frequency.

study of cyanide-ligated protoglobin mutants revealed that the low g_z values could in that case be associated with a higher admixture of the d_{xy} orbital in the singularly occupied molecular orbital (SOMO) containing the unpaired electron, due to the extreme ruffling of the haem in these proteins [31]. This ruffling is reflected by the hyperfine values of the haem nitrogens, which are different among each other and at least one is as low as 3.9 MHz (in absolute value). This is not the case for NGB-CN and H64QNGB-CN for which the haem ^{14}N hyperfine and

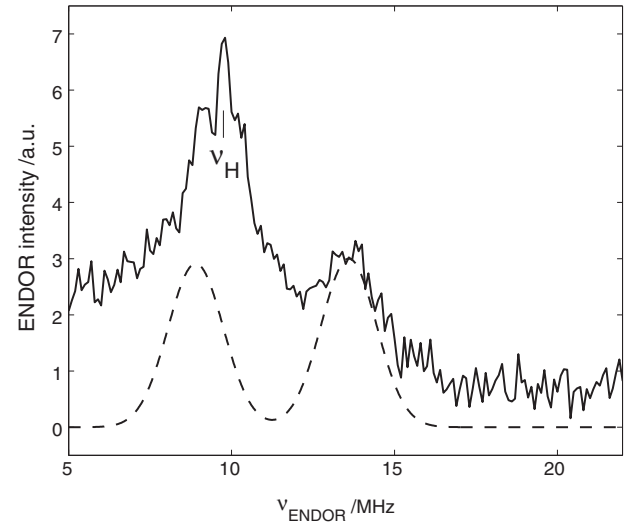

Fig. 4. Experimental (solid) and simulated (dashed) X-band Davies ENDOR spectra taken at an observer position corresponding with g_z of a frozen solution of ferric NGB-^{13}CN. The simulations are computed using parameters given in Table 2. ν_H indicates the position of the proton Larmor frequency.

nuclear quadrupole values (Table 3) and the corresponding HYSCORE cross-peaks are very similar to those observed for hhMb-CN [31]. Hence, the lower g_z value of the cyanide complexes of the NGB variants in this study cannot stem from haem ruffling effects. Although ruffling may be different in the ferric and ferrous forms of a globin, the fact that no severe haem ruffling was found for the CO-complex of ferrous mNgb (Fig. 6a) [17] in contrast to the haem ruffling observed in O_2-ligated ferrous protoglobin variants [51] seems to support this conclusion.

When comparing the principal g values of wild-type NGB-CN with the two protein samples with point mutations at positions E7 and B10 (H64QNGB-CN and F28LNGB-CN, resp.), we observe a clear influence of the point mutations. While ferric wt NGB and F28LNGB are in a low-spin ferric state due to the bis-histidine ligation of the heme iron [8,15,16], ferric H64QNGB is characterized by a high-spin state of the ferric iron with an absence of a distal ligand [37]. However, inspection of Table 1 shows that there is no obvious relationship between the coordination of the ferric haem iron in the absence of exogenous ligands on the one hand and the principal g values after cyanide ligation on the other hand.

Another possible factor that could affect the g_z values of the cyanide complexes is the amino acids at positions E7 and B10, which are known to play a crucial role in ligand binding in mammalian myoglobins [52,53]. The E7 position has, for instance, shown to be important for NO-ligation to NGB. The EPR parameters (g values and ^{14}N hyperfine values) of NO-ligated ferrous NGB and H64QNGB were found to be clearly different, reflecting the difference in ligand stabilization by the E7(64) residue [54]. The temperature dependence of the EPR spectra of ferrous NGB-NO was also markedly different from that of hhMb-NO, reflecting an altered influence of the His64 residue on the NO ligand coordination [54]. Surprisingly, the X-ray structure of CO-ligated ferrous mNgb shows the imidazole plane of E7His to be oriented in such a way that hydrogen bonding to the ligand is not possible (Fig. 6a, [17]). It is at present not known whether this is also the case for the corresponding cyanide or NO complexes. In fact, resonance Raman data showed the co-existence of two conformations of the Fe–CO unit in CO-ligated mNgb, one arising from an open conformation of the haem pocket in which CO is not interacting with any nearby residue and one in which a positively charged residue stabilizes the CO ligand (probably the E7His) [10]. The above observations for the CO- and NO-ligated neuroglobins make it likely that, at least to some extent, the amino acids at position E7 influences the EPR parameters of the cyanide complexes of globins.

Only limited EPR data on cyanide complexes of globins having Gln at position E7 have been reported (Table 1). Interestingly, the g_z values of these cyanide-ligated proteins are very close to those found here for the H64QNGB-CN complex. The X-ray crystallographic structures of cyanide-ligated *Lp*Hb I [55] and *Chlam*Hb [56] reveal strong hydrogen bonding between the cyanide nitrogen and the Gln at E7 (see also Table 4). Similarly, the NMR analysis of the cyanide complex of the H64Q/V68F double point mutant of mNgb shows that Gln64 is in a position to form a hydrogen bond with the cyanide ligand [22]. It is therefore very likely that this is also a feature in the H64QNGB-CN complex under study. If the His64 imidazole in NGB-CN is indeed oriented as in mNgb-CO [17], the decrease in the g_z value of H64QNGB-CN could be related to the formation of stronger hydrogen bonds with the cyanide ligand, which will pull the electron (spin density) away from the metal and cyanide ligand.

The Phe28 residue at position B10 is in turn found to play a crucial role in transmitting the structural information from the disulfide bridge to the haem-pocket region [16] and to be essential in the ligand migration between internal docking sites in photodissociated carbon-monoxy mNgb [57,58]. The PheB10 ligand in CO-ligated ferrous mNgb is found to be situated very near to the CO ligand and in van der Waals contact with CO (Fig. 6a, [17]), a position that is retained in the cyanide complex of the H64Q/V68F double mutant of mNgb [22]. Mutation to the smaller

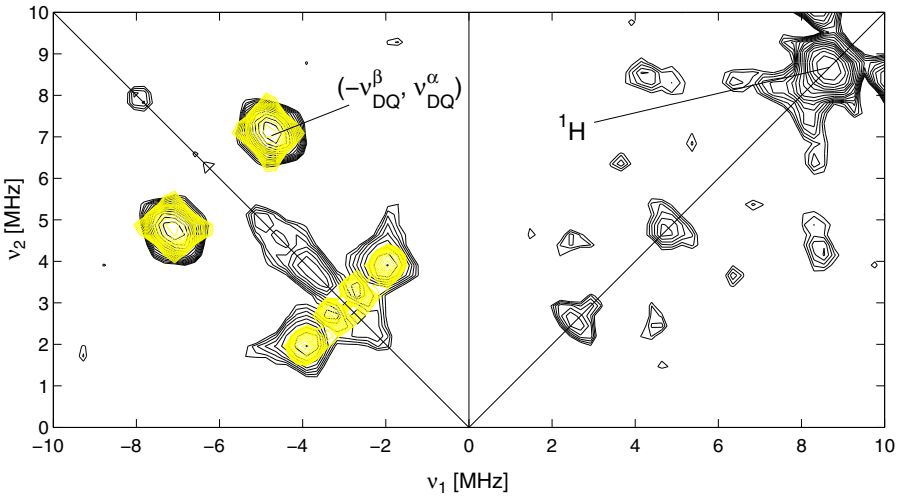

Fig. 5. Black: Experimental X-band SMART HYSCORE spectrum of a frozen solution of ferric H64QNGB-CN recorded at an observer position corresponding with g_z. Yellow: corresponding simulation of the haem ^{14}N contribution (Table 3). The double-quantum (DQ) cross-peaks are indicated.

Leu residue removes these van der Waals contacts, which may influence the cyanide ligand stabilization.

Another way to explain the very different values of g_z for NGB-CN might be by considering the work of Fujii et al. [32–35], who have tried to explain trends in ^{13}C NMR shifts of ^{13}CN-bound heme proteins in terms of a "push" and a "pull" effect. Unfortunately, their work showed some shortcomings in the theoretical treatment, as will be shown in the following. The very low g_z value observed for the cyanide complexes of haem oxygenases and peroxidases (Table 1) has been associated with the imidazolate character of the proximal His side chain mediated by the hydrogen bonding of the proximal imidazole NH protons with nearby aspartate or glutamate residues [46,47]. Fujii and et al. have linked this hydrogen bonding to the observed ^{13}C NMR shift of the cyanide carbon [32–35]. In reference [33], they predicted the A_x and A_y values of the ^{13}C hyperfine tensor of the cyanide carbon in swMb-CN to be $A_x = A_y = -52.6$ MHz, a prediction made on the basis of the ^{13}C NMR shift and the A_z hyperfine value determined earlier by Mulks et al. ([26], Table 2). Our current results on hhMb-CN (Table 2) show that this prediction is not supported by the experimental data (hhMb-CN and swMb-CN have almost identical g, $A_z(^{13}C)$ and ^{13}C NMR shifts, so the full ^{13}C hyperfine tensors will be very close in magnitude). To understand the large discrepancy between the predicted and experimental values, it is worth looking at the derivation employed by Fujii and Yoshida [33]. The observed ^{13}C NMR shift of swMb-CN ($\delta = -4145$ ppm from tetramethylsilane) was considered to be composed of a diamagnetic shift (estimated to be $+177$ ppm on the basis of the NMR shift of $K_2Fe(CN)_6$), and a residual shift of -4322 ppm, which in turn is the sum of a contact shift, δ_{con}, and a dipolar shift, δ_{dip}. The dipolar shift ($+409$ ppm) was calculated from

$$\delta_{dip} = \frac{\mu_0}{4\pi}\beta^2 \frac{S(S+1)}{9kT}\left\{\left(g_z\text{-}\frac{g_x^2+g_y^2}{2}\right)\left(\frac{3\cos^2\theta\text{-}1}{R^3}\right)+\frac{3}{2}\left(g_x^2\text{-}g_y^2\right)\left(\frac{\sin^2\theta\cos 2\phi}{R^3}\right)\right\} \quad (1)$$

with R the C_{CN}–Fe distance (2.02 Å), β the Bohr magneton, μ_0 the permittivity of free space and θ and ϕ determine the orientation of the nucleus–metal axis in the molecular frame ($\theta = 0°$ for the carbon of cyanide). This expression is valid if only the ground-state contribution needs to be considered and all excited states can be ignored [41,49,50,59,60]. It has been known for a long time that this is not valid for cyanide complexes of haem proteins [49,59], for which the first excited state is contributing to a large extent at room temperature. Errors induced by neglecting these contributions for low-spin d^5 configurations can easily amount to over 20% [60]. Furthermore, Eq. (1) assumes that a point-dipole approximation is valid, *i.e.* that the unpaired electron can be assumed to be at the position of the iron nucleus. This approximation is valid for large Fe-nucleus distances, but is very likely not to hold for the directly coordinating cyanide carbon. This will introduce a further error.

The resulting δ_{con} (-4731 ppm) obtained after subtraction of δ_{dip} was then linked by Fujii and Yoshida [33] to the isotropic hyperfine value using the McConnell expression [61]

$$\delta_{con} = A_{iso}\frac{|\gamma_e|}{|\gamma_N|}\frac{S(S+1)}{3kT}. \quad (2)$$

This expression not only ignores the effect of the g-anisotropy (*i.e.* the spin-orbit contribution), the expression is only valid for a single electron in an orbital which is well separated from any other excited level [50], which is definitely not the case for any of the cyanide-ligated haem proteins [49,59]. At room temperature a significant population of the excited states would need to be taken into account. A final error in the derivation of the $A_{x,y}$ values was introduced by assuming that the anisotropic part of the hyperfine tensor can be represented as $[-T\ -T\ 2T]$, which ignores the g-anisotropy effect and additional p-orbital contributions.

Fujii and coworkers [33–35] linked the changes in the ^{13}C NMR shifts of the cyanide carbons in CN-haem complexes to so-called push and pull effects. If the extent of hydrogen bonding to the proximal imidazole

Table 3
^{14}N-hyperfine and nuclear quadrupole couplings of the haem nitrogens of cyanide-ligated neuroglobins determined by HYSCORE spectroscopy of frozen solutions. The values are compared with reported data on cyanide-ligated haem proteins.

	$\lvert A_{zz}\rvert$/MHz	$\lvert P_{zz}\rvert$/MHz[a]	Reference
NGB-CN	5.2/5.8[b] ± 0.1	0.4 ± 0.1	This work
H64QNGB-CN	5.8/6.0 ± 0.1	0.3 ± 0.1	This work
hhMb-CN	5.8/6.1	0.4	[31]
F145WPgb*-CN	3.9–5.6	0.2	[31]
swMb-CN	5.84/6.36	0.6/0.58	[26]
Cyt P450-CN	5.2/5.9	0.27	[36]

[a] This represents the nuclear quadrupole value along the haem normal, which is not the dominant axis of the quadrupole tensor (largest quadrupole principal value).
[b] '/' indicates the presence of two different contributions with different parameters.

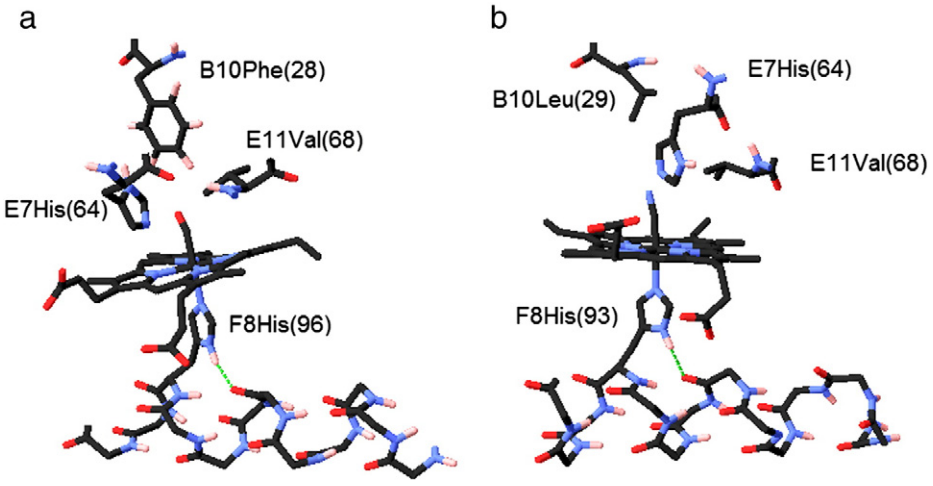

Fig. 6. Comparison between the haem structure of (a) CO-ligated ferrous mNgb (PDB 1W92 [17]) and (b) cyanide-ligated ferric swMb (PDB 2JHO [62]). The hydrogen bond between the backbone of the F α-helix and the proximal F8His is shown with dashed lines. The haem structure is represented such that the top part is the distal side of the haem.

NH increases (more imidazolate character of the proximal His), the binding of cyanide becomes weaker due to the trans effect, resulting in less effective electron spin transfer from the heme iron to the coordinated cyanide. This increased push effect will decrease the ^{13}C NMR shifts. Furthermore, the hydrogen-bonding to the distal cyanide nitrogen pulls the electron density from the cyanide atoms and also leads to a decrease of the ^{13}C NMR shift, although to a lesser extent than caused by the push effect. This relation was derived on the basis of comparing cyanide-ligated haem proteins and model complexes with known large imidazolate character of the proximal His (*e.g.* due to strong hydrogen bonding of the NH to an aspartate or glutamate) and cases with much weaker hydrogen bonding (*e.g.* to backbone carbonyls). Noteworthy is that none of the latter proteins used for comparison involved haem proteins with weak hydrogen bonding to the proximal His and g_z values below 3.4, such as the NGB cases or many other globins mentioned in Table 1.

Although the ^{13}C-hyperfine tensor components could only partially be determined for NGB-CN and H64QNGB-CN, it is already clear that they differ significantly from the ones of hhMb-CN (on average a reduction by 15% of the resolved components). This indicates a change in the electron spin density on the ^{13}C nucleus which will also lead to a significant change in the ^{13}C NMR shift. Although no X-ray crystallographic data is to date available of cyanide-ligated neuroglobins, neither the structure of ferric wild-type NGB [9] or the one of CO-ligated mNgb [17] show strong hydrogen bonding to the proximal His (Fig. 6a). In fact, all the cyanide-ligated globins cited in Table 1 for which a crystal structure is available exhibit only weak hydrogen bonding of the proximal histidine to a backbone carbonyl (indicated in Fig. 6 for both NGB-CO and swMb-CN). In Table 4, relevant structural data are shown for a number of cyanide-ligated globins in comparison to CO-ligated mNgb. The only apparent trend between the structural parameters and the g_z value seems to be the distance between the proximal imidazole nitrogen and the nearest carbonyl oxygen. hHb-CN and swMb-CN have a longer N_{His}–$O_{carbonyl}$ distance. This will influence the hydrogen bonding to the proximal imidazole, but this influence is expected to be far less than that of the presence of Asp or Glu residues in the peroxidases. Nevertheless, the ^{13}C-NMR shift was found to decrease only in the range of 8–18% from swMb-CN to different cyanide-ligated peroxidases and oxygenases, which is in the order of the decrease in the carbon hyperfine value observed here between ferric swMb-CN and (H64Q)NGB-CN. This indicates that factors other than the imidazolate character of the proximal His can influence the ^{13}C spin density. In fact, Fujii et al. [35] already noticed that although point mutation of Asp to Asn or Ala led to an increase of the ^{13}C NMR shift (due to reduction or removal of the hydrogen bond), the shifts were still much smaller than the ones observed for the cyanide complexes of myoglobin and haemoglobin. They suggested that differences in the location of the helix containing the proximal His may also play a role, an argument that may be important in the NGB case in view of the observed haem sliding effects (Fig. 6a [17]).

Finally, in their analysis of the cyanide ^{13}C-hyperfine tensor of ferric cyanide-ligated cytochrome P450cam, Hoffman and co-workers used a simple heuristic bonding model [36] in which the Fe–C–N angle (α) is related to the isotropic hyperfine coupling. Since the isotropic coupling stems from the s-orbital spin density in the sp^n hybrid orbital on carbon, the hybridization of the sp^n orbital can be linked with α and the isotropic hyperfine coupling A_{iso} is then

$$\frac{A_{iso}(\alpha)}{A_{iso}(\alpha=\pi)} = \frac{\cos\alpha}{\cos\alpha - 1}. \quad (3)$$

In a very crude approximation, where we assume that all cyanide-ligated globins would have the same $A_{iso}(\alpha=\pi)$ constant, the decrease in the isotropic hyperfine value of the NGB-CN complexes versus that of

Table 4
Selected relevant structural parameters of cyanide-ligated globins in comparison to CO-ligated ferrous mNgb. All distances are given in Å.

	g_z of cyanide complex	Distance proximal $N_{His}-O{=}C_{carbonyl}$	Distance Fe–$N_{His,proximal}$	Distance Fe–C_{ligand}	Distance between N or O of ligand and N of His or Gln at E7	PDB source [reference]
swMb-CN	3.442	3.03	2.08	1.92	2.96	2JHO [62]
hHb-CN	3.41	3.11	1.93	2.08	2.62	1ABY [63]
Barley Hb-CN	3.32	2.66	2.09	2.84	2.62	2OIF [64]
*Lp*Hbl-CN	3.29	2.90	2.13	1.95	3.00	1B0B [55]
*Chlam*Hb-CN	3.19	2.71	2.18	2.65	2.92[a]	1DLY [56]
mNgb-CO	3.295[b]	2.76	2.11	1.81	3.20	1W92 [17]

[a] B10Tyr oxygen is at 2.36 Å from cyanide nitrogen.
[b] Value for NGB-CN is taken.

hhMb-CN would stem from a decrease in the Fe–C–N angle. This angle is 167° in the 2JHO PDB structure of swMb-CN (Fig. 6b). Fujii and Yoshida [33] considered the effects of the Fe–C–N angle on the ^{13}C NMR shifts to be minor. They supported their conclusion by the fact that the reported X-ray crystallographic study of hhMb-CN reveals a value of $\alpha = 137°$, while hhMb-CN and swMb-CN have very similar ^{13}C NMR shifts. However, one has to be very careful in interpreting Fe–C–N angles obtained from X-ray crystallographic data. It has been shown that the haem iron can be reduced by the X-rays [55]. The Fe(II)–CN has a structure with a far lower α value than an Fe(III)–CN unit [55]. On the other hand, the Fe–C–N angle may be different at low temperature (EPR conditions) than at room temperature (NMR) conditions. It will therefore be important to perform systematic ^{13}C-NMR, EPR and ENDOR for a series of cyanide complexes of globins and other haem proteins with varying *g* values (and preferably existing crystallographic structures), so as to be able to characterize all structural parameters that govern the ^{13}C(cyanide) magnetic interactions as well as the ***g*** tensor of these systems. These systems also form a challenge for modern-day quantum-chemical computations.

Information about the magnitude of the push effect follows also from ^{15}N NMR shifts of the cyanide nitrogen [33–35]. Attempts to determine the corresponding hyperfine tensor by EPR techniques failed, as the contributions are masked by the haem and His nitrogen contributions [31].

5. Conclusion

The electronic structure of the haem active site controls its reactivity and propensity to coordinate and stabilize ligands, with the protein's electronic structure being finely tuned by residues close to the active site. In this study, large differences in the electron Zeeman interaction (*g*-values) between the ferric cyanide complexes of wild-type human neuroglobin (NGB) and its H64Q and F28L point mutants and the ones of the cyanide complexes of mammalian myoglobin and haemoglobin were observed. Davies ENDOR enabled for the first time the determination of the full ^{13}C hyperfine tensor of the cyanide carbon ligated to horse heart myoglobin (hhMb). Disagreement of these experimental parameters with earlier predictions based on ^{13}C NMR [33] revealed significant shortcomings in the theoretical model employed in [33] to describe the magnetic couplings. Using Davies ENDOR, a partial determination of the ^{13}C hyperfine tensor of the cyanide carbon in cyanide-ligated NGB and H64QNGB could be obtained. Again, significant differences were observed compared to the hhMb-CN case.

A thorough analysis of the current findings in relation to reported EPR, NMR and X-ray data of different cyanide-ligated ferric haem proteins revealed that a multitude of factors influence the magnetic parameters. While hydrogen binding to the proximal imidazole NH (push effect) was earlier put forward as the main explanation for ^{13}C NMR shift of the cyanide carbons in CN–haem complexes [33–35], this effect cannot explain the significant differences observed in the EPR data of cyanide-ligated globins. Indeed, all globins show only weak hydrogen bonding between the proximal His NH and a backbone carbonyl. The main difference between the cyanide-ligated forms of mammalian myoglobin and haemoglobin and of the neuroglobin proteins seems to be the degree of stabilization/hydrogen bonding between the cyanide and the side chain of the residue at position E7 and the Fe–C–N angle. Our earlier investigation of cyanide-ligated protoglobin variants [31] also indicated haem ruffling as another important factor that can influence the magnetic parameters. This effect can however be excluded for the neuroglobin cases under study.

The magnetic data presented in this study, both *g*-values and hyperfine couplings, along with the existing NMR and X-ray data provide a means to test and develop theoretical models of how the electronic structure in cyanide-ligated haem proteins is fine-tuned by the protein's binding pocket.

Abbreviations

*Chlam*Hb	*Chlamydomonas* haemoglobin
Cyt	cytochrome
*Dm*Hb	*Drosophila melanogaster* haemoglobin
DQ	double quantum
ENDOR	electron nuclear double resonance
EPR	electron paramagnetic resonance
HALS	highly anisotropic low spin
Hb	haemoglobin
hHb	human haemoglobin
hhMb	horse heart myoglobin
HTA	high turning angle
*Lp*Hb	*Lucina pectinata* haemoglobin
Mb	myoglobin
MD	molecular dynamics
NP4	*Drosophila melanogaster* haemoglobin
mNgb	murine neuroglobin
Ngb	neuroglobin
NGB	human neuroglobin
Pgb*	Cys → Ser mutant of protoglobin
NMR	nuclear magnetic resonance
sb legHb	soyabean leghaemoglobin

Acknowledgements

SVD acknowledges support from the Hercules Foundation, Flanders (contract AUHA013). SVD and SD also thank the Fund for Scientific Research – Flanders (FWO) (grant G.0687.13) and the GOA-BOF UA 2013–2016 (project-ID 28312) for funding. JH acknowledges financial support from the ARC/FT120100421.

Appendix A. Supplementary data

Supplementary data to this article can be found online at http://dx.doi.org/10.1016/j.bpc.2014.03.007.

References

[1] T. Burmester, B. Weich, S. Reinhardt, T. Hankeln, A vertebrate globin expressed in the brain, Nature 407 (2000) 520–523.
[2] S.L. Milton, G. Nayak, P.L. Lutz, H.M. Prentice, Gene transcription of neuroglobin is upregulated by hypoxia and anoxia in the brain of the anoxia-tolerant turtle Trachemys scripta, J. Biomed. Sci. 13 (2006) 509–514.
[3] J. Dröge, A. Pande, E.W. Englander, W. Makałowski, Comparative genomics of neuroglobin reveals its early origins, PLoS ONE 7 (2012) e47972.
[4] C. Awenius, T. Hankeln, T. Burmester, Neuroglobins from the Zebrafish *Danio rerio* and the pufferfish *Tetraodon nigroviridis*, Biochem. Biophys. Res. Commun. 287 (2001) 418–421.
[5] A. Pesce, M. Bolognesi, A. Bocedi, P. Ascenzi, S. Dewilde, L. Moens, T. Hankeln, T. Burmester, Neuroglobin and cytoglobin, fresh blood for the vertebrate globin family, EMBO Rep. 3 (2002) 1146–1151.
[6] C.H. Cheng, P.G. di, C. Verde, The "icefish paradox." Which is the task of neuroglobin in Antarctic hemoglobin-less icefish? IUBMB Life 61 (2009) 184–188.
[7] T. Burmester, T. Hankeln, What is the function of neuroglobin? J. Exp. Biol. 212 (2009) 1423–1428.
[8] S. Dewilde, L. Kiger, T. Burmester, T. Hankeln, V. Baudin-Creuza, T. Aerts, M.C. Marden, R. Caubergs, L. Moens, Biochemical characterization and ligand binding properties of neuroglobin, a novel member of the globin family, J. Biol. Chem. 276 (2001) 38949–38955.
[9] A. Pesce, S. Dewilde, M. Nardini, L. Moens, P. Ascenzi, T. Hankeln, T. Burmester, M. Bolognesi, Human brain neuroglobin structure reveals a distinct mode of controlling oxygen affinity, Structure 11 (2003) 1087–1095.
[10] M. Couture, T. Burmester, T. Hankeln, D.L. Rousseau, The heme environments of mouse neuroglobin: evidence for the presence of two conformations of the heme pocket, J. Biol. Chem. 276 (2001) 36377–36382.
[11] J.T. Trent III, R.A. Watts, M.S. Hargrove, Human neuroglobin, a hexacoordinate haemoglobin that reversibly binds oxygen, J. Biol. Chem. 276 (2001) 30106–30110.
[12] S. Van Doorslaer, S. Dewilde, L. Kiger, S.V. Nistor, E. Goovaerts, M.C. Marden, L. Moens, Nitric oxide binding properties of neuroglobin: a characterization by EPR and flash photolysis, J. Biol. Chem. 278 (2003) 4919–4925.
[13] D. Hamdane, L. Kiger, S. Dewilde, B.N. Green, A. Pesce, J. Uzan, T. Burmester, T. Hankeln, M. Bolognesi, L. Moens, M.C. Marden, The redox state of the cell regulates

the ligand binding affinity of human neuroglobin and cytoglobin, J. Biol. Chem. 278 (2003) 51713–51721.
[14] D. Hamdane, L. Kiger, S. Dewilde, J. Uzan, T. Burmester, T. Hankeln, L. Moens, M.C. Marden, Hyperthermal stability of neuroglobin and cytoglobin, FEBS J. 272 (2005) 2076–2084.
[15] E. Vinck, S. Van Doorslaer, S. Dewilde, L. Moens, Structural change of the heme pocket due to disulfide bridge formation is significantly larger for neuroglobin than for cytoglobin, J. Am. Chem. Soc. 126 (2004) 4516–4517.
[16] M. Ezhevskaya, F. Trandafir, L. Moens, S. Dewilde, S. Van Doorslaer, EPR investigation of the role of B10 phenylalanine in neuroglobin — evidence that B10Phe mediates structural changes in the heme region upon disulfide-bridge formation, J. Inorg. Biochem. 105 (2011) 1131–1137.
[17] B. Vallone, K. Nienhaus, A. Matthes, M. Brunori, G.U. Nienhaus, The structure of carbonmonoxy neuroglobin reveals a heme-sliding mechanism for control of ligand affinity, Proc. Natl. Acad. Sci. 101 (2004) 17351–17356.
[18] M. Anselmi, M. Brunori, B. Vallone, A. Di Nola, Molecular dynamics simulation of the neuroglobin crystal: comparison with the simulation in solution, Biophys. J. 95 (2008) 4157–4162.
[19] J. Xu, G. Yin, W. Du, Distal mutation modulates the heme sliding in mouse neuroglobin investigated by molecular dynamics simulation, Proteins 79 (2011) 191–202.
[20] W. Du, R. Syvitski, S. Dewilde, L. Moens, G.N. La Mar, Solution ^{1}H NMR characterization of equilibrium heme orientational disorder with functional consequences in mouse neuroglobin, J. Am. Chem. Soc. 125 (2003) 8080–8081.
[21] W.-H. Du, G.-W. Yin, Y.-J. Li, Q. Wei, J. Li, W.-H. Fang, Ligand binding affinity of cyanide complex of single mutant F106L murine met-neuroglobin, Chem. J. Chin. Univ. 28 (2007) 1547–1551.
[22] G. Yin, Y. Li, J. Li, J. Li, W. Du, Q. Wei, W. Fang, Solution ^{1}H NMR study of the active site structure for the double mutant H64Q/V6F cyanide complex of mouse neuroglobin, Biophys. Chem. 136 (2008) 115–123.
[23] A. Bocahut, V. Derrien, S. Bernad, P. Sebban, S. Sacquin-Mora, E. Guittet, E. Lescop, Heme orientation modulates hisitdine dissociation and ligand binding kinetics in the hexacoordinated human neuroglobin, J. Biol. Inorg. Chem. 18 (2013) 111–122.
[24] J. Xu, L. Li, G. Yin, W. Du, Ligand orientation of human neuroglobin obtained from solution NMR and molecular dynamics simulation as compared with X-ray crystallography, J. Inorg. Biochem. 103 (2009) 1693–1701.
[25] H. Hori, Analysis of the principal g tensors in single crystals of ferrimyoglobin complexes, Biochem. Biophys. Acta 251 (1971) 227–235.
[26] C.F. Mulks, C.P. Scholes, L.C. Dickinson, A. Lapidot, Electron Nuclear Double Resonance from high- and low-spin ferric hemoglobins and myoglobins, J. Am. Chem. Soc. 101 (1979) 1645–1654.
[27] C.A. Appleby, W.E. Blumberg, J. Peisach, B.A. Wittenberg, J.B. Wittenberg, Leghemoglobin: an electron paramagnetic resonance and optical spectral study of the free protein and its complexes with nicotinate and acetate, J. Biol. Chem. 251 (1976) 6090–6096.
[28] M. Couture, T.K. Das, H.C. Lee, J. Peisach, D.L. Rousseau, B.A. Wittenberg, J.B. Wittenberg, M. Guertin, Chlamydomonas chloroplast ferrous hemoglobin: heme pocket structure and reactions with ligands, J. Biol. Chem. 274 (1999) 6898–6910.
[29] T.K. Das, H.C. Lee, S.M.G. Duff, R.D. Hill, J. Peisach, D.L. Rouuseau, B.A. Wittenberg, J.B. Wittenberg, The heme environment in Barley hemoglobin, J. Biol. Chem. 274 (1999) 4207–4212.
[30] D.W. Kraus, J.B. Wittenberg, L. Jing-Fen, J. Peisach, Hemoglobins of the Lucina pectinata/Bacteria symbiosis. II. An electron paramagnetic resonance and optical spectral study of the ferric proteins, J. Biol. Chem. 265 (1990) 16054–16059.
[31] S. Van Doorslaer, L. Tilleman, B. Verrept, F. Desmet, S. Maurelli, F. Trandafir, L. Moens, S. Dewilde, Marked difference in the electronic structure of cyanide-ligated ferric protoglobins and myoglobin due to heme ruffling, Inorg. Chem. 51 (2012) 8834–8841.
[32] H. Fujii, ^{13}C NMR signal detection of iron-bound cyanide ions in ferric cyanide complexes of heme proteins, J. Am. Chem. Soc. 124 (2002) 5936–5937.
[33] H. Fujii, T. Yoshida, ^{13}C and ^{15}N NMR studies of iron-bound cyanides of heme proteins and related model complexes: sensitive probe for detecting hydrogen-bonding interactions at the proximal and distal sides, Inorg. Chem. 45 (2006) 6816–6827.
[34] D. Nonaka, H. Wariishi, H. Fujii, Paramagnetic ^{13}C and ^{15}N NMR analyses of cyanide-(^{13}C^{15}N-) ligated ferric peroxidases: The push effect, not pull effect, modulates the compound I formation rate, Biochemistry 48 (2009) 898–905.
[35] D. Nonaka, H. Wariishi, K.G. Welinder, H. Fujii, Paramagnetic ^{13}C and ^{15}N NMR analyses of the push and pull effects in cytochrome c peroxidase and Coprinus cinereus peroxidase variants: functional roles of highly conserved amino acids around heme, Biochemistry 49 (2010) 49–57.
[36] T.-C. Yang, R.L. McNaughton, M.D. Clay, F.E. Jenney Jr., R. Krishnan, D.M. Kurtz Jr., M.W.W. Adams, M.K. Johnson, B.M. Hoffman, Comparing the electronic properties of the low-spin cyano-ferric [Fe(N4)(Cys)] active sites of superoxide reductase and P450cam using ENDOR spectroscopy and DFT calculations, J. Am. Chem. Soc. 128 (2006) 16566–16578.
[37] F. Trandafir, P. ter Heerdt, M. Fittipaldi, E. Vinck, S. Dewilde, L. Moens, S. Van Doorslaer, Studying high-spin ferric heme proteins by pulsed EPR spectroscopy: analysis of the ferric form of the E7Q mutant of human neuroglobin, Appl. Magn. Reson. 31 (2007) 553–572.
[38] L. Liesum, A. Schweiger, Multiple quantum coherence in HYSCORE spectra, J. Chem. Phys. 114 (2001) 9478–9488.
[39] E.R. Davies, New pulse ENDOR technique, Phys. Lett. A 47 (1974) 1–2.
[40] S. Stoll, A. Schweiger, EasySpin, a comprehensive software package for spectral simulation and analysis in EPR, J. Magn. Chem. 178 (2006) 42–55.
[41] F.A. Walker, Magnetic spectroscopic (EPR, ESEEM, Mössbauer, MCD and NMR) studies of low-spin ferriheme centers and their corresponding heme proteins, Coord. Chem. Rev. 185–186 (1999) 471–534.
[42] R.G. Shulman, S.H. Glarum, M. Karplus, Electronic structure of cyanide complexes of hemes and heme proteins, J. Mol. Biol. 57 (1971) 93–115.
[43] J. Qin, G.N. La Mar, F. Ascoli, M. Brunori, Solution nuclear magnetic resonance determination of active site structure for a paramagnetic protein: cyanomet Aplysia myoglobin, J. Mol. Biol. 231 (1993) 1009–1023.
[44] T. Shokhireva, A. Weichsel, K.M. Smith, R.E. Berry, N.V. Shokhirev, C.A. Balfour, H. Zhang, W.R. Monfort, F.A. Walker, Assignment of the ferriheme resonances of the low-spin complexes of nitrophorins 1 and 4 by 1H and 13C NMR spectroscopy: comparison to structural data obtained from X-ray crystallography, Inorg. Chem. 46 (2007) 2041–2056.
[45] D.L. Brautigan, B.A. Feinberg, B.M. Hoffman, E. Margoliash, J. Peisach, W.E. Blumberg, Multiple low spin forms of the cytochrome c ferrihemochrome. EPR spectra of various eukaryotic and prokaryotic cytochromes c, J. Biol. Chem. 252 (1977) 574–582.
[46] M. Ikeda-Saito, S. Kimura, Axial ligand coordination in intestinal peroxidase, Arch. Biochem. Biophys. 283 (1990) 351–355.
[47] W.E. Blumberg, J. Peisach, B.A. Wittenberg, J.B. Wittenberg, The Electronic structure of protoheme proteins. I. An electron paramagnetic resonance and optical study of horseradish peroxidise and its derivatives, J. Biol. Chem. 243 (1968) 1854–1862.
[48] J.S. Griffith, On the magnetic properties of some haemoglobin complexes, Proc. Roy. Soc. London 235 (1956) 23–36.
[49] W.D. Horrocks, E.S. Greenberg, Evaluation of dipolar nuclear magnetic resonance shifts in low-spin hemin systems: ferricytochrome c and metmyoglobin cyanide, Biochim. Biophys. Acta 322 (1973) 38–44.
[50] I. Bertini, C. Luchinat, G. Parigi, Magnetic susceptibility in paramagnetic resonance, Prog. Nucl. Magn. Reson. Spectrosc. 40 (2002) 249–273.
[51] M. Nardini, A. Pesce, L. Thijs, J.A. Saito, S. Dewilde, M. Alam, P. Ascenzi, M. Coletta, C. Ciaccio, L. Moens, M. Bolognesi, Archaeal protoglobin structure indicates new ligand diffusion paths and modulation of haem-reactivity, EMBO Rep. 9 (2008) 157–163.
[52] T.E. Carver, R.E. Brantley Jr., E.W. Singleton, R.M. Arduini, M.L. Quillin, G.N. Phillips, J.S. Olson, A novel site-directed mutant of myoglobin with an unusually high O2 affinity and low autooxidation rate, J. Biol. Chem. 267 (1992) 14443–14450.
[53] A. Bracaccio, F. Cutruzzolá, C. Travaglini Allocatelli, M. Brunori, S.J. Smerdon, A.J. Wilkinson, Y. Dou, D. Keenan, M. Ikeda-Saito, R.E. Brantley Jr., J.S. Olon, Structural factors governing azide and cyanide binding to mammalian metmyoglobins, J. Biol. Chem. 269 (1994) 13843–13853.
[54] F. Trandafir, S. Van Doorslaer, S. Dewilde, L. Moens, Temperature dependence of NO binding modes in human neuroglobin, Biochim. Biophys. Acta 1702 (2004) 153–161.
[55] M. Bolognesi, C. Rosano, R. Losso, A. Borassi, M. Rizzi, J.B. Wittenberg, A. Boffi, P. Ascenzi, Cyanide binding to Lucina pectinata haemoglobin I and sperm whale myoglobin: an x-ray crystallographic study, Biophys. J. 77 (1999) 1093–1099.
[56] A. Pesce, M. Couture, S. Dewilde, M. Guertin, K. Yamauchi, P. Ascenzi, L. Moens, M. Bolognesi, A novel two-over-two α-helical sandwich fold is characteristic of the truncated hemoglobin family, EMBO J. 19 (2000) 2424–2434.
[57] K. Nienhaus, G.U. Nienhaus, Influence of distal residue B10 on CO dynamics in myoglobin and neuroglobin, J. Biol. Phys. 33 (2007) 357–370.
[58] S. Lutz, K. Nienhaus, G.U. Nienhaus, M. Meuwly, Ligand migration between internal docking sites in photodissociated carbonmonoxy neuroglobin, J. Phys. Chem. B 113 (2009) 15334–15343.
[59] I. Bertini, C. Luchinat, G. Parigi, Hyperfine shifts in low-spin iron(III) hemes: a ligand field analysis, Eur. J. Inorg. Chem. (2000) 2473–2480.
[60] B.R. McGarvey, N.C. Batista, C.W.B. Bezerra, M.S. Schultz, D.W. Franco, 1H NMR and EPR studies of $[M(NH_3)_5(H_2O)](TFMS)_3$ (M = Ru, Os). Theory of paramagnetic shift for strong field d5 complexes, Inorg. Chem. 37 (1998) 2865–2872.
[61] H.M. McConnell, D.B. Chesnut, Theory of isotropic hyperfine interactions in pi-electron radicals, J. Chem. Phys. 28 (1958) 107–117.
[62] A. Arcovito, M. Benfatto, M. Cianci, S.S. Hasnain, K. Nienhaus, G.U. Nienhaus, C. Savino, R.W. Strange, B. Vallone, S. Della Longa, X-ray structure analysis of a metalloprotein with enhanced active-site resolution using in situ x-ray absorption near edge structure spectroscopy, Proc. Natl. Acad. Sci. U. S. A. 104 (2007) 6211–6216.
[63] K.S. Kroeger, C.E. Kundrot, Structures of a hemoglobin-based blood substitute: insights into the function of allosteric proteins, Structure 5 (1997) 227–237.
[64] J.A. Hoy, H. Robinson, J.T. Trent III, S. Kakar, B.J. Smagghe, M.S. Hargrove, Plant hemoglobins: a molecular fossil record for the evolution of oxygen transport, J. Mol. Biol. 371 (2007) 168–179